# Boron Diffusion and Activation in Silicon in the Presence of Other Species

Hong-Jyh Li [*,**], Puneet Kohli [*], Swaroop Ganguly [*], Taras A. Kirichenko [*], Peter Zeitzoff [**], Kenneth Torres [**] and Sanjay Banerjee [*]

[*] Microelectronics Research Center, University of Texas at Austin
10100 Burnet Road, MER 1.108, R9900, TX 78712, hong_jyh_li@mail.utexas.edu
[**] International SEMATECH, 2706 Montopolis Drive, Austin, TX 78741, peter.zeitzoff@sematech.org

## ABSTRACT

Modeling and experimental investigation of B equilibrium diffusivity and its activation in Si in the presence of other species, including *ab initio* calculations, are presented here. The results suggest that incorporating other species along with B into the Si substrate can achieve shallower junctions and higher B activation in semiconductor device applications.

***Keywords***: Boron, Diffusion, Activation, Shallow Junction, *ab initio* Calculation

## 1. INTRODUCTION

As semiconductor device technology evolves, shallower junction depth ($X_j$) and lower sheet resistance ($R_s$) are projected [1]. Particularly for 70nm and below technology nodes, $X_j$ and $R_s$ requirements place severe restrictions on the ion-implantation and annealing technologies. Transient enhanced diffusion (TED)[2] of B due to ion implantation damage poses severe challenges to the reduction of junction depth. It is found that B diffusivity can be enhanced substantially above the equilibrium value, depending on the implantation and annealing condition [3]. As is well known, TED is caused by the non-equilibrium Si interstitial concentration. The enhanced B diffusivity $D_B^{enh}$ is to a good approximation given by [2]

$$D_B^{enh} = D_B^* \frac{[I]}{[I^*]} , \qquad (1)$$

where $D_B^*$ denotes the B diffusivity under equilibrium conditions, $[I^*]$ is the equilibrium interstitial concentration, and TED is encompassed in the $\frac{[I]}{[I^*]}$ factor. Previous modeling [4] has focused on the impact of TED, in effect ignoring any variation of $D_B^*$ in the above equation. However, there is evidence that $D_B^*$ can be reduced by the use of co-implants with B, thereby providing a potential pathway to achieving shallow $p^+$-n junctions with low sheet resistance. In this paper, the impact on B diffusivity of using co-implants to affect $D_B^*$ is explored. *Ab initio* calculations of the migration energy of B in the presence of other species such as F, N, C, Ge, B, Al, Ga, and In are presented, and shown to be consistent with experimental B diffusion results. In addition, simulations and experimental evidence indicate that both the total and electrically active B concentration can be higher in the presence of larger atomic size acceptors. Prior work on B diffusion in the presence of N/Ge/F/B is shown in the Table I

TABLE I
Summary for the prior work on B diffusion in the presence of N, Ge, F, and B

| Species | Ref. | Effect | Why (from authors) |
|---|---|---|---|
| N | 5 | D(B) decrease (PolySi) | B-N complex |
| F | 9 | D(B) decrease | Unclear |
| Ge | 6 | D(B) decrease | $I^*$ decreased by Ge |
| C | 8 | D(B) decrease | I decreased by C |
| B | 10 | D(B) increase | I increased by silicon boride |

*: Silicon interstitials

## 2. B MIGRATION ENERGY SIMULATION

So far, the generation and recombination of excess Si interstitials explain most of the experimental results relating to TED. However, in the Ge, C and BED cases, there is evidence that the equilibrium B diffusivity, $D_B^*$, is decreased (or enhanced). In those cases, Si excess interstitials are probably not the only cause, because the diffusion reduction or enhancement has been observed in chemical vapor deposition (CVD) and molecular beam epitaxy (MBE) prepared samples where Si interstitial concentration is at its equilibrium value [2]. To investigate the behavior of $D_B^*$, we used the efficient plane-wave ultrasoft pseudopotential code, Vienna *Ab Initio* Simulation Package (VASP)[11]. The simulations were performed in a uniform grid of k points equivalent to a 3 X 3 X 3 Monkhorst and Pack grid in the diamond cubic cell. The energy calculation was performed in a 64-atom unit cell. The smaller supercell gives errors of a few percent in the relative defect energy [4]. Here we adopt the interstitial diffusion mechanism to study the equilibrium B diffusion, where the Hexagonal-Tetragonal path is presumably the main migration pathway for B interstitials [12]. The B is located in the [110] channel and the 64 atoms located at the substitutional sites are comprised of 63 Si atoms and one test species (Fig. 1).

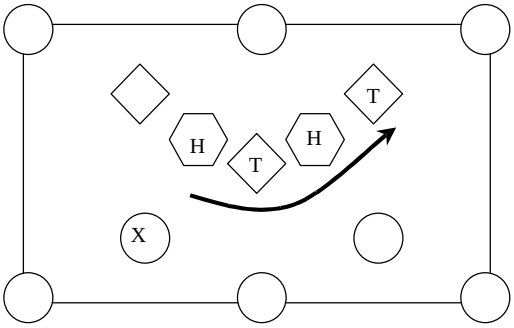


Fig. 1. Illustration of the simulation structure ((110) plane) in this work. The X position is where we put the test species. The symbols ○ ◇ ⬡ represent the substitutional, tetragonal and hexagonal sites, respectively.

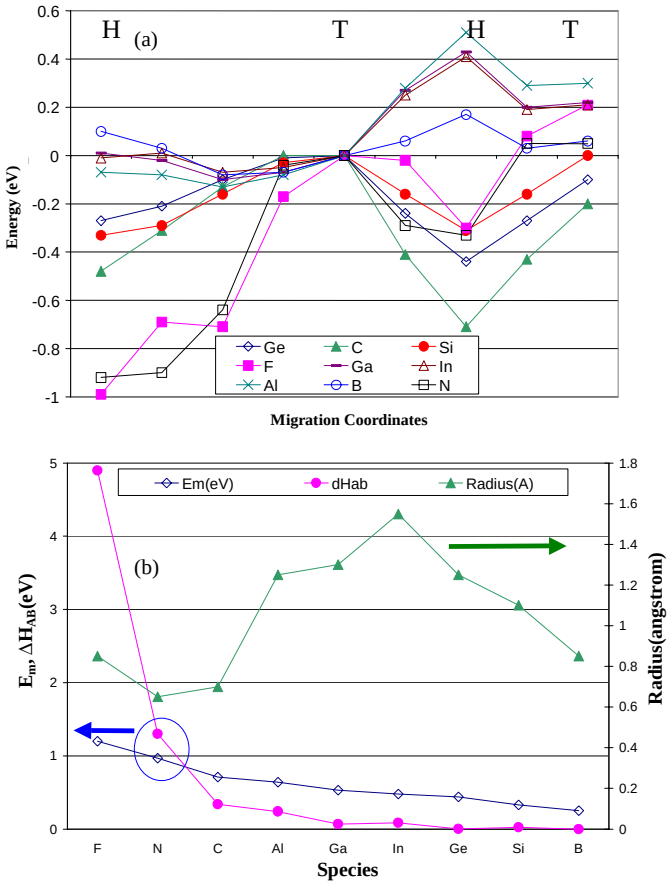


Fig. 2. (a) 1-D energy profiles connecting H-T-T pathway with either Si or test species in the X position, as shown in Fig. 1. The energies shown here are relative to the energy at the central T site. Here the X is for F, N, Ge, C, Al, Ga, In, B, and Si. (b) $\Delta H_{AB}$ , the enthalpy of bond formation between atoms A and B, as well as $E_m$ , migration energy, and atomic size.

In this way, the coordinates of B are fixed and the surrounding 64 atoms relax to the minimum energy configuration. Hence, as B is placed at different positions the pathway (successive H, T, H, T sites along the arrow in Fig. 1), we can calculate the energy profile associated with the pathway. These simulated profiles are shown in Fig. 2(a) for the various test species. The B migration energy, $E_m$, is the difference between the minimum and maximum energies along the pathway, and is plotted in Fig. 2(b) and listed in Table II.

TABLE II

Simulated $E_m$ for different X atoms. For X=F/N/C/Al/Ga/In/Ge, B diffusivity is expected to be lower due to higher $E_m$ than X=Si case, and the diffusivity for X=B case is expected to be larger. All these are qualitatively consistent with experiments.

| X | Migration Energy ($E_m$) (eV) |
|---|---|
| F | 1.20 |
| N | 0.97 |
| C | 0.71 |
| Al | 0.64 |
| Ga | 0.53 |
| In | 0.48 |
| Ge | 0.44 |
| Si | 0.33 |
| B | 0.25 |

Those test species for which $E_m$ is larger than the reference value (0.33 eV for B and Si) can be expected to cause less B diffusion than the pure B case; otherwise, if $E_m$ is smaller than 0.33 eV, the diffusion should be larger. Furthermore, these effects on the diffusivity are expected only at large concentrations of the test species where a non-negligible fraction of the unit cells has a test species atom. The simulation results are consistent with the experimental facts from the literature cited in the previous section. Fluorine ($E_m$=1.2 eV), N ($E_m$ =0.97 eV), C ($E_m$ =0.71 eV) and Ge ($E_m$ =0.44 eV) all cause decreased diffusion, while with B ($E_m$ = 0.25eV) there is enhanced diffusion (BED). For F, aside from the impact of the Si interstitials reduction presented in [9], $D_B^*$ should also be reduced by the F incorporation because of its high $E_m$. For N, the simulation result of high migration energy agrees with the experimental observation of formation of immobile B-N complex. In addition to the test species mentioned above (F, N, C, Ge, and B), we performed simulations and experiments with Al, Ga and In. Since those atoms are also in column III in the periodic table, they are expected to provide extra holes, which should lower the sheet resistance in ultra-shallow junctions. The simulation results for $E_m$ are consistent with our experimental results, as shown below.

## 3. EXPERIMENTS FOR X=Al/Ga/In

We first grow a layer of $SiO_2$ (150A) on top of a Si wafer and co-implant Al, Ga, In and $BF_2$ in different combinations, as shown in Table III. The $SiO_2$ layer acts as an out-diffusion source for the co-implanted atoms in the succeeding annealing process. The SIMS profiles after anneal are shown in Fig. 3. Also, the depth at which each profile has a concentration of $1x10^{18}$ $cm^{-3}$ is listed. It shows that B diffusion has been reduced by the co-implanted species, which is consistent with our simulation results. In addition, as the total dose of co-

implanted species increases (i.e. for the cases where two or all three species are co-implanted), the reduction is more pronounced. This is similar to the effect reported in [5, 6, 7, 8, 9, and 10] where it is observed that the reduction of B diffusion (or increase as in the BED case) is more pronounced when the concentration of the other species is increased. In our model, this can be explained by the increasing chances for the B to pass along a channel with other species in the neighborhood when the dose of those species is increased.

TABLE III.
Design of experiment for co-implanted $BF_2$, Al, Ga, and In samples. After co-implantation, some samples are annealed at 1050 C for 10 seconds and the others are annealed at 950 for 30 seconds, as explained later. The $BF_2$ implant conditions are 10keV, $2x10^{15}$ $cm^{-2}$ except for the cases of 3.5BF and 3BF that are 10keV, 3.5 $x10^{15}$ $cm^{-2}$ and 10keV, 3.0 $x10^{15}$ $cm^{-2}$ respectively. The implant conditions for Al, Ga, and In are 5keV, $1x10^{15}$ $cm^{-2}$, 9keV, $1x10^{15}$ $cm^{-2}$, and 11keV, $1x10^{15}$ $cm^{-2}$ respectively.

| Samples | Implant species combinations | | | |
|---|---|---|---|---|
| B-reference | $BF_2$ | | | |
| B-Al | $BF_2$ | Al | | |
| B-Ga | $BF_2$ | | Ga | |
| B-In | $BF_2$ | | | In |
| B-Al-Ga | $BF_2$ | Al | Ga | |
| B-Ga-In | $BF_2$ | | Ga | In |
| B-Al-Ga-In | $BF_2$ | Al | Ga | In |
| 3.5BF | $BF_2$ | | | |
| 3BF | $BF_2$ | | | |

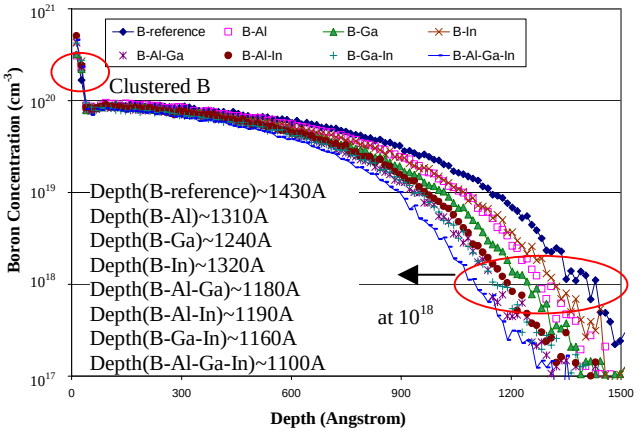


Fig. 3. Boron SIMS result (annealed at 1050C, 10s) for co-implantation with Al, Ga, and In followed by out-diffusion from a $SiO_2$ layer into Si. The implant matrix is shown in Table III.

Physically, the reasons for the difference between the B migration energies in the presence of different test species can be understood as an interplay of strain and electronic effects. The strain caused by the misfit of Si and the test species increases system energy. On the other hand, the electronic bonding between B and the test species decreases the system energy so that the $E_m$ increases in the case of strong bonding. The chemical bonds become increasingly ionic in character as the difference in the electronegativities of the ligands increases. Conversely, bonds between atoms with similar or equal values of electronegativities tend to be covalent or metallic in nature. To be precise, the enthalpy of bond formation between atoms A and B for an ionic bond can be approximately expressed as [13]

$$\Delta H_{ionic} = k(\chi_A - \chi_B)^2 , \qquad (2)$$

where $\chi_A$ and $\chi_B$ are electronegativities for atoms A and B. $k$ is empirically found to be 1.3 eV. With this approximation, we plot the enthalpy of the bond between B and the test species, atomic sizes and the $E_m$ in Fig. 2(b). The electronic effect (bonding) is generally dominant when the enthalpy is large (from F to Al in Fig. 2(b)), whereas the strain effect is significant when the enthalpy is small (from Ga to B in Fig. 2(b)).

## 4. ENERGY OF $B_S$-$X_S$ PAIR (X=Al/Ga/In/Si/B)

The atomic arrangement in this simulation is shown in Fig. 4. We calculate the energy (E(B-X)) when B and X are located together at the substitutional sites denoted by Bs-Xs (Fig. 4(a)) and the energy (E(B- -X)) in which case B and X are separated by one lattice constant (c) apart, as denoted by Bs- -Xs and shown in Fig. 4(b). If E(X-B)< E(X- -B), then X and B tend to cluster together and X plays the role of B getter. We can compare the values of E(X-B)-E(X- -B) and E(B-B)-E(B- -B) where $X \neq B$ If the former is larger, then the presence of X should increase the B solubility. In addition, E(B-X-B) and E(B-X- -B) are also calculated, where another B atom replaces the substitutional Si which is the nearest neighbor of the X atom. In this case, we can compare the value of E(B-X-B)-E(B-X- -B) where X=Si and B, and the values where X=Al, Ga, and In. The result is plotted in Fig. 5. In addition to provide additional holes, the larger acceptor atoms (Al/Ga/In) act as B getters and hence increase the B solubility. Therefore, higher carrier concentration is expected in this case. Interestingly, B-Ga has a positive energy whereas B-Al has a negative one. This could be due to the effect of electronegativity difference between Ga-B and Al-B, as explained in Fig. 2(b)

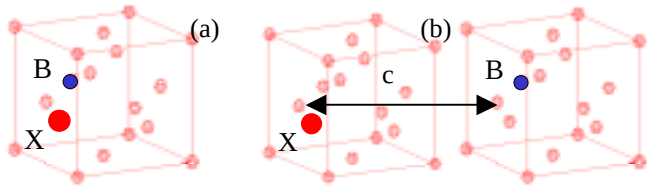


Fig. 4. Atomic arrangement in the simulation of Bs-Xs pair. The empty circles are Si atoms, bigger solid circle is X and smaller solid circle is B. (a) is the case for Bs-Xs configuration. (b) is the case for Bs--Xs where B is located a lattice constant away, as in (a).

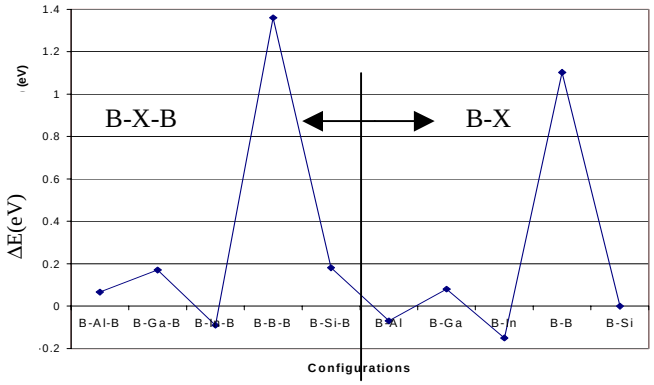


Fig. 5 Energy difference, ΔE, between Bs-Xs and Bs--Xs or between Bs-X-Bs and Bs-Xs--Bs configurations. The data shown over here implies that B can dissolve more in the substrate with X incorporation than in the case without X.

## 5. SIMS/SRP RESULTS

The experimental design is shown in Table III and the SIMS (Secondary Ion Mass Spectrometry) /SRP (Spreading Resistance Profile) results are plotted in Fig. 6 in which we note that the profiles for 3BF/3.5BF are very similar, suggesting that at 950C/30s, B peak concentration reaches its solubility limit at this annealing condition. The increase in peak carrier concentrations for B-Ga-In cannot be explained as the sum of the carriers coming from the co-implant species, because the differences in peak carrier concentrations observed are much more than the peak atomic concentrations of the co-implant species. A comparison of the SIMS profiles of these samples clearly indicates an increase in the B peak concentration, thus confirming the electronic and strain-compensation effects.
We note that the carrier concentration near the surface for 3.5BF is much less than that of the B-Ga-In case.

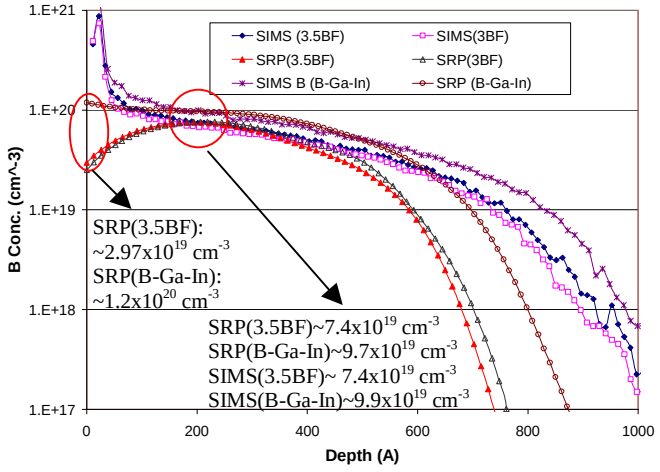


Fig. 6 SIMS/SRP results for the selected experiments (annealed by 950C, 30s) in Table II. Note that the peak concentration of B and carrier concentration for B-Ga-In is much larger than 3BF/3.5BF indicating more B can be soluble (and activated) in the Ga-In incorporated substrate although B cluster exists near the surface.

## 6. SUMMARY

We model B diffusion and activation for the equilibrium case in the presence of other species with *ab initio* simulation. The result shows that in the presence of other atoms X (X= F, N, C, Al, Ga, In, Ge), the migration energy for B along the migration pathway is larger than the case if X = Si. This suggests the reduction of B diffusion. If another B occupies that position (X= B) then a smaller migration energy is observed and enhanced diffusion is expected. The simulation results are consistent with experiments. A*b initio* simulations also indicate that the equilibrium B concentration can be higher in the presence of the larger acceptors. Along with the contribution of holes from the other acceptors (Al/Ga/In), a lower sheet resistance can be expected. The reason for the migration and $B_s$-$X_s$ pair energy difference can be understood in terms of electronic and strain effects. SIMS and SRP results confirm the above theoretical implications. Therefore, incorporating other acceptors along with B into a Si substrate can be a feasible method to achieve shallower junctions, and lower sheet resistance in semiconductor device applications.
This work was supported in part by the SRC-FEP Center, and TATRP.

## REFERENCES

[1] *National Technology Roadmap for Semiconductors* (Semiconductor Industry Association, San Jose, CA, 1999).
[2] P. M. Fahey, B. P. Griffin, and J. D. Plummer. Rev. Mod. Phys. 61, 289 (1989).
[3] P. A. Stolk, H.-J. gossmann, D. J. Eaglesham, D. C. Jacobson, C. S. Rafferty, G. H. Gilmer, M. Jaraiz, J. M. Poate, H. S. Luftman, and T. E. Haynes, Appl. Phys. Lett. 81, 6031 (1997); A. Agarwal, H.-J. Gossmann, D. J. Eaglesham, L. Pelaz, D. C. Jacobson, T. E. Haynes, and Y. E. Erokhin, Appl. Phys. Lett. 71, 3141 (1997)
[4] Jing Zhu, Tomas Diaz dela Rubia, L. H. Yang, Christian Mailhiot, and George H. Gilmer, Phys. Rev. B 54, 4741 (1996); B. Sadigh, T. J. Lenosky, S. K. Theiss, M-J. Caturla, T. D. de la Rubia, and M. A. Foad, Phys. Rev. Lett. 83, 4341 (1999). W. Windl, M. M. Bunea, R. Stumpf, S. T. Dunham, and M. P. Masquelier, Phys. Rev. Lett. 83, 4345 (1999)
[5] T. S. Chao, M. C. Liaw, C. H. Chu, C. Y. Chang, C. H. Chien, C. P. Hao, and T. F. Lei, Appl. Phys. Lett. 69, 1781 (1996)
[6] T. T. Fang, W. T. C. Fang, P. B. Griffin, and J. D. Plummer, Appl. Phys. Lett., 68, 791 (1996)
[7] P. Kuo, J. L. Hoyt, J. F. Gibbons, J. E. Turner, and D. Lefforge, Mat. Res. Soc. Symp. Proc. 379. 378 (1995)
[8] H. Rücker, B. Heinemann, W. Röpke, R. Kurps, D. Krüger, G. Lippert, and H. J. Osten, Appl. Phys. Lett., 73, 1682 (1998)
[9] D. F. Downey, J. W. Chow, E. Ishida, and K. S. Jones, Appl. Phys. Lett. 73, 1263 (1998)
[10] A. Agarwal, H.-J. Gossmann, D. J. Eaglesham, S. B. Herner, A. T. Fiory, and T. E. Haynes, Appl. Phys. Lett. 74, 2435 (1999)
[11] G. Kresse and J. Hafner, Phys. Rev. B 47, 558 (1993); 49, 14251 (1994); Phys. Rev. B 54, 11169 (1996).
[12] H. C. Casey, Jr. and G. L. Pearson, in *Point Defects in Solids Vol. II*, edited by J. H. Crawford, Jr. and L. M. Slifkin (Plenum Press, New York and London, 1975), p. 22
[13] R. J. Borg, and G. J. Dienes, The Physical Chemistry of Solids, (Academic, San Diego, 1992), p. 156